



NIRSpec Technical Note NTN-2013-006

Author(s): G. Giardino & G. De Marchi
Date of Issue: September 18, 2013
Version: 1.0

European Space Research
and Technology Centre
Keplerlaan 1
2201 AZ Noordwijk
The Netherlands
Tel. (31) 71 5656565
Fax (31) 71 5656040
www.esa.int

Monitoring of closed micro shutters during NASA MSA tests

Abstract:

During Cycle 2 of the Performance Verification and Calibration campaign (CPV) of NIRSpec flight module 2 (FM2), NASA MSA team performed a series of tests of NIRSpec micro shutter array (MSA) in secondary park position. In this note we provide a summary of the monitoring of the number of closed micro shutters during these test sequences.

1 INTRODUCTION

During Cycle 2 of the Performance Verification and Calibration campaign (CPV) of NIRSpec flight module 2 (FM2), NASA MSA team performed a series of tests with the NIRSpec micro-shutter array (MSA) in Secondary park position. The aim of the tests was the reduction of the emission ('glow') from shorted micro-shutters when the MSA is in secondary park position. The tests were subdivided in two main phases: 'functional' tests and 'performance' tests. During the performance tests, dark exposures were acquired to assess the level of emission from shorted micro-shutters; the result of analysis of these dark exposures will be described in a separate document. In this document we summarize the results of the analysis of the number of closed shutters in each MSA quadrant during the performance tests.

Two main test sequences — repeated a number of times during the functional and performance tests — were executed: one long sequence of 20 exposures, of which 19 are illuminated exposures, and one short sequence of 8 exposures, of which 7 are illuminated. As source, the NIRSpec internal CAA lamp TEST was used. All the exposures were reduced with the ESA pre-processing pipeline (Birkmann 2011) to derive count-rate images; these images were then analyzed with the software package *MSA-detect* (Giardino 2012) to derive the number of closed shutters in each MSA quadrant in every illuminated exposure.

During the functional part of the tests, the MSA temperature decreased from 66 K to 52 K. However, the exposures with a checkerboard pattern needed to establish the alignment between MSA and detector pixels were only acquired at the beginning and at the end of this phase. Over this range of temperatures, we see the MSA-detector alignment changes sig-

nificantly (by approximately 1.5 pixel). Since *MSA-detect* relies on the coordinate transform between the MSA plane and the detector plane derived from the checkerboard exposures, and this transform is changing significantly during the functional tests, the automated identification of closed shutters by the software is not completely reliable during the set of functional tests. Therefore, in this note, we summarize only the results from the exposures acquired during the performance phase.

The performance MSA tests started on 1 Aug 2013 (day 213), when the checkerboard exposure (MSA-CHK-173) was acquired, and continued until the morning of 2 Aug (day 214). During this period the MSA temperature changed from 52 K to 45 K and the MSA-detector alignment changed by less than 0.3 pixel, without impacting the accuracy of *MSA-detect*.

2 RESULTS FOR LONG TEST SEQUENCES

During the performance phase, two 20-exposure sequences were performed, respectively named: NRS_SPG-13 and NRS_SPG-16 (see the Appendix for a complete list of the exposures and directory names). In Fig. 1 the number of failed closed shutters for each quadrant during these tests is given as a function of the test number.

In the following figures (2 – 5) the images of each MSA quadrant acquired in the first exposure of each of the two test sequence are shown. From the figures, one can easily see that the higher number of closed shutters during sequence SPG-13 are due to a higher number of masked rows and columns in this test sequence compared to SPG-16.

Note that to better see these details it is necessary to enlarge the figures in the electronic version of this document. If more detail is needed, we can provide higher resolution images, in PDF format, and also the original count-rate frames. If required, count rate mages and results from *MSA-detect* for the functional part of the tests are also available.

3 RESULTS FOR SHORT TEST SEQUENCE

During the performance phase of the MSA tests only one short test sequence was successfully completed, namely SPG-15. The number of closed shutters for each quadrant during this test sequence are summarised in Fig. 6. During this sequence, the number of closed shutters remains essentially constant for all quadrants but quadrant 3, for which at test number 4 the number of closed shutters increases by approximately 600. Fig. 7 provides a comparison between images of quadrant 3 in the first and last exposure of this test sequence.

REFERENCES

Birkmann, S. 2011, Description of the NIRSpec pre-processing pipeline, NIRSpec Technical Note NTN-2011-004, ESA/ESTEC available at <http://www.cosmos.esa.int/web/jwst/technical-notes>

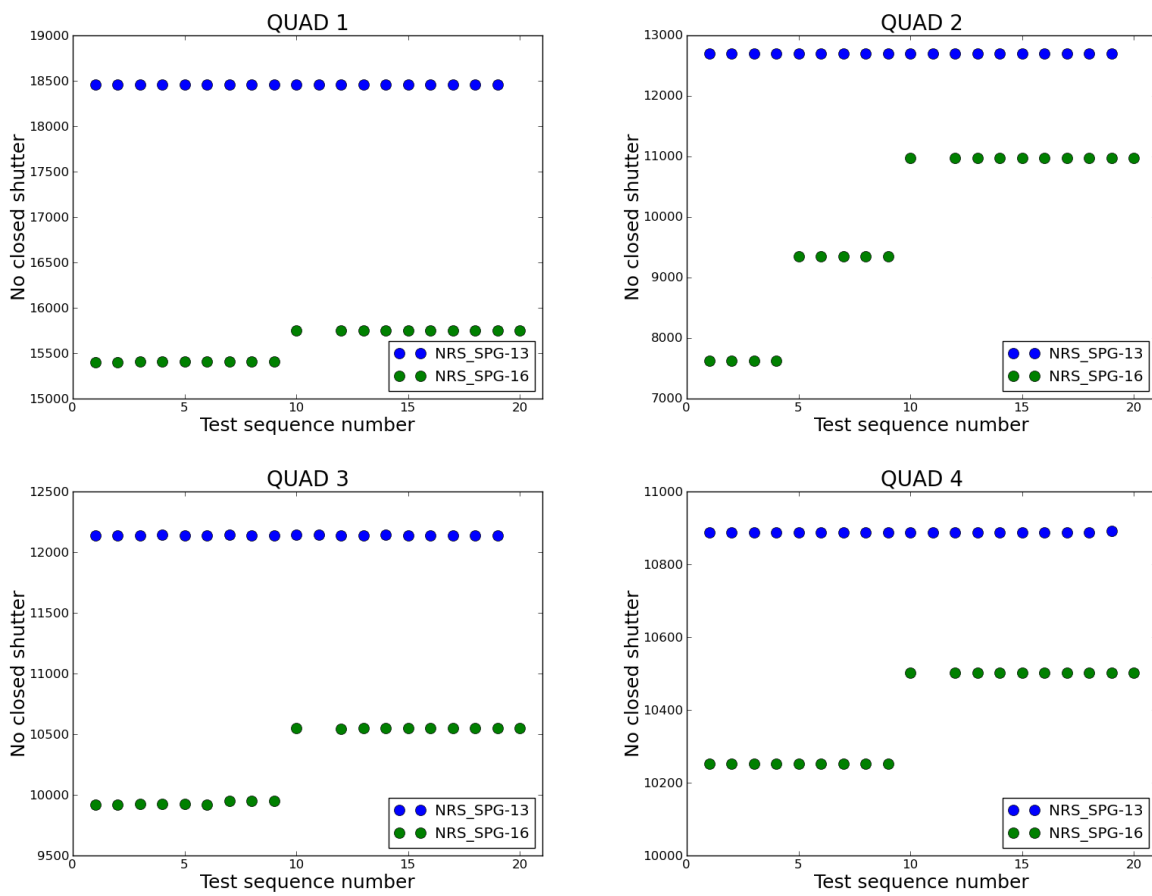


Figure 1: Number of closed shutters in each MSA quadrant as a function of the exposure number within the two test sequences: SPG-13 and SPG-16.

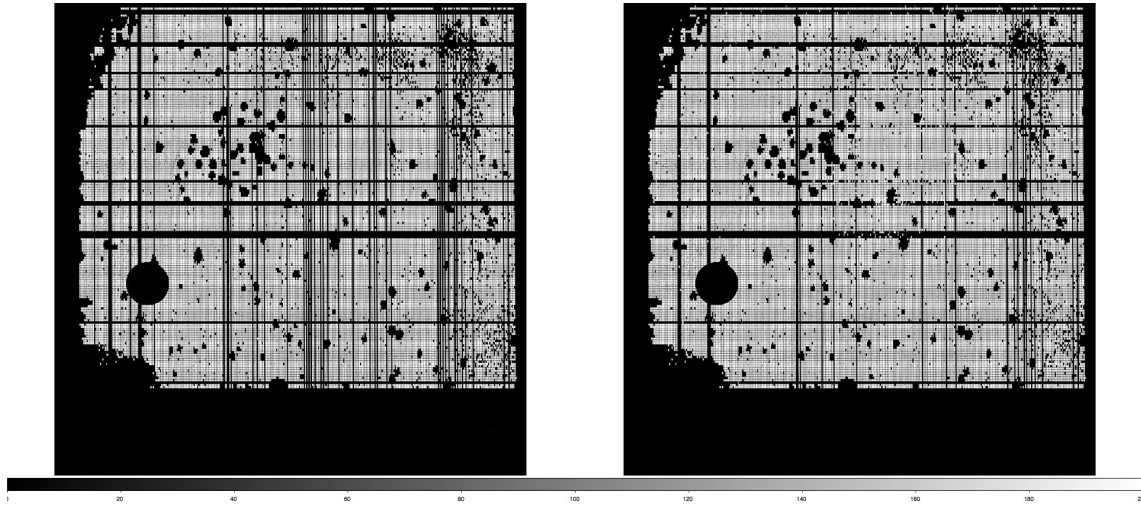


Figure 2: Quadrant 1 image in exposures SPG-13-1-Q0-PP-A-Init (left) and SPG-16-1-Q0-PP-A-Init (right).

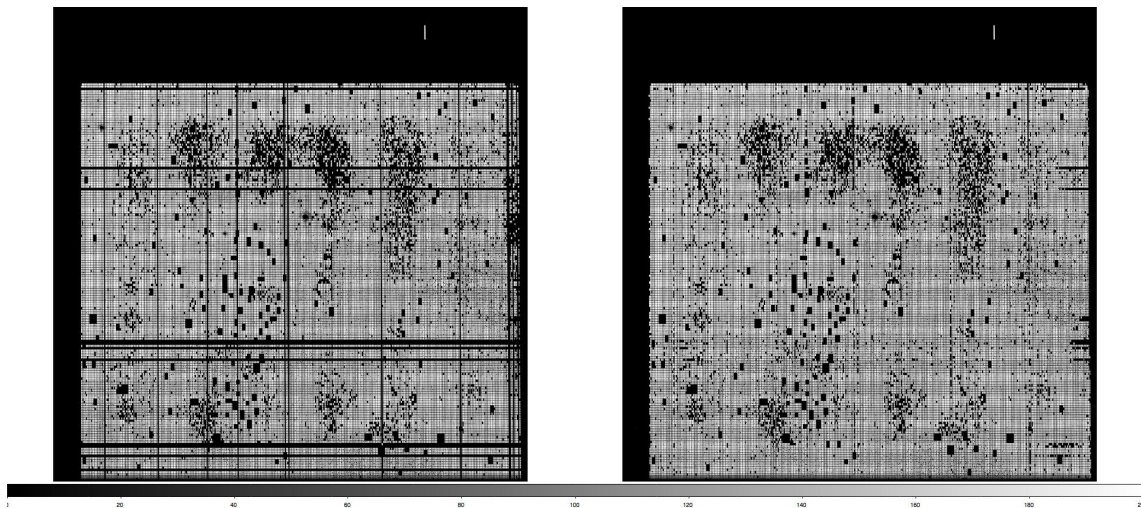


Figure 3: Quadrant 2 image in exposures SPG-13-1-Q0-PP-A-Init (left) and SPG-16-1-Q0-PP-A-Init (right).

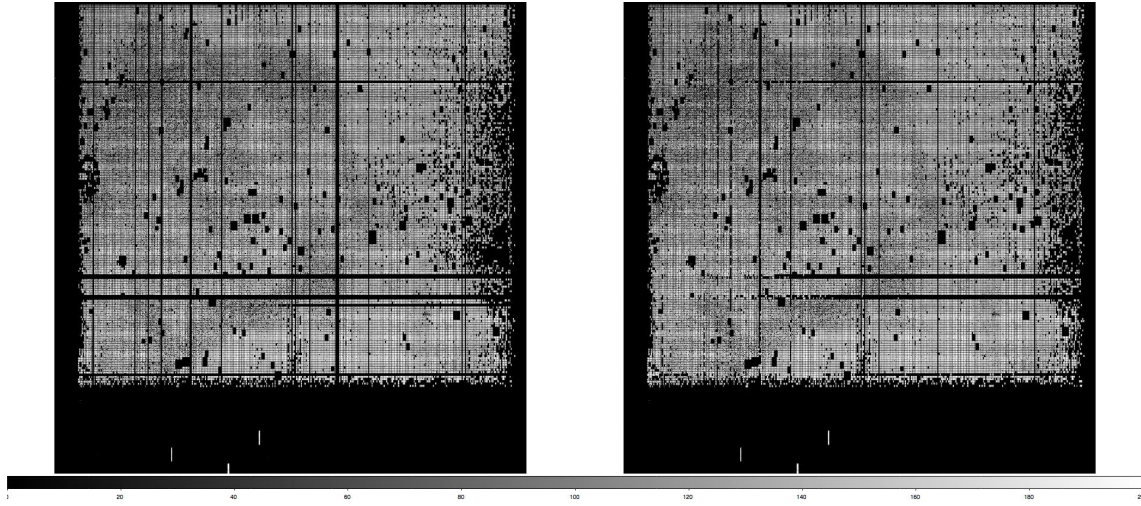


Figure 4: Quadrant 3 image in exposures SPG-13-1-Q0-PP-A-Init (left) and SPG-16-1-Q0-PP-A-Init (right).

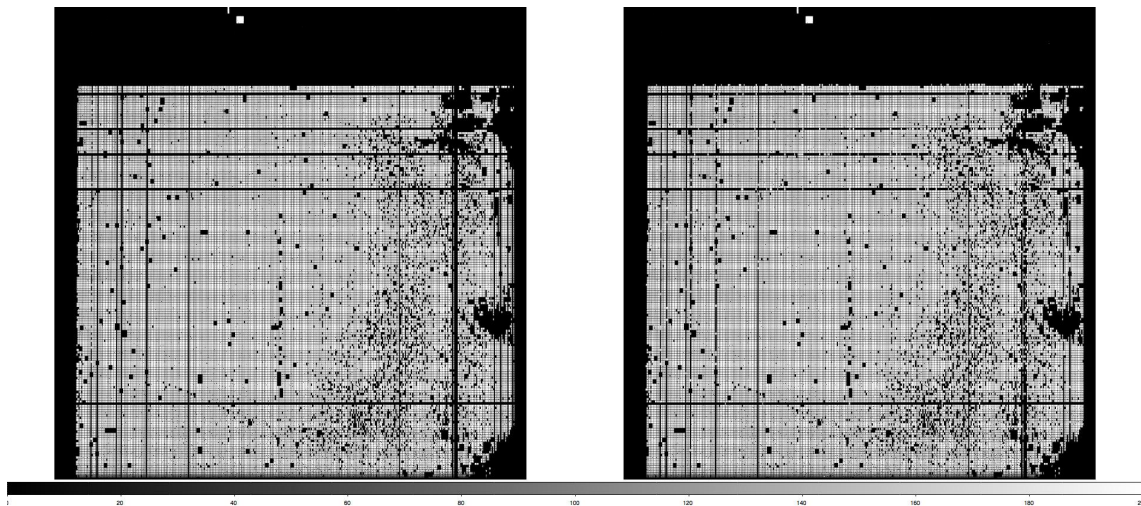


Figure 5: Quadrant 4 image in exposures SPG-13-1-Q0-PP-A-Init (left) and SPG-16-1-Q0-PP-A-Init (right).

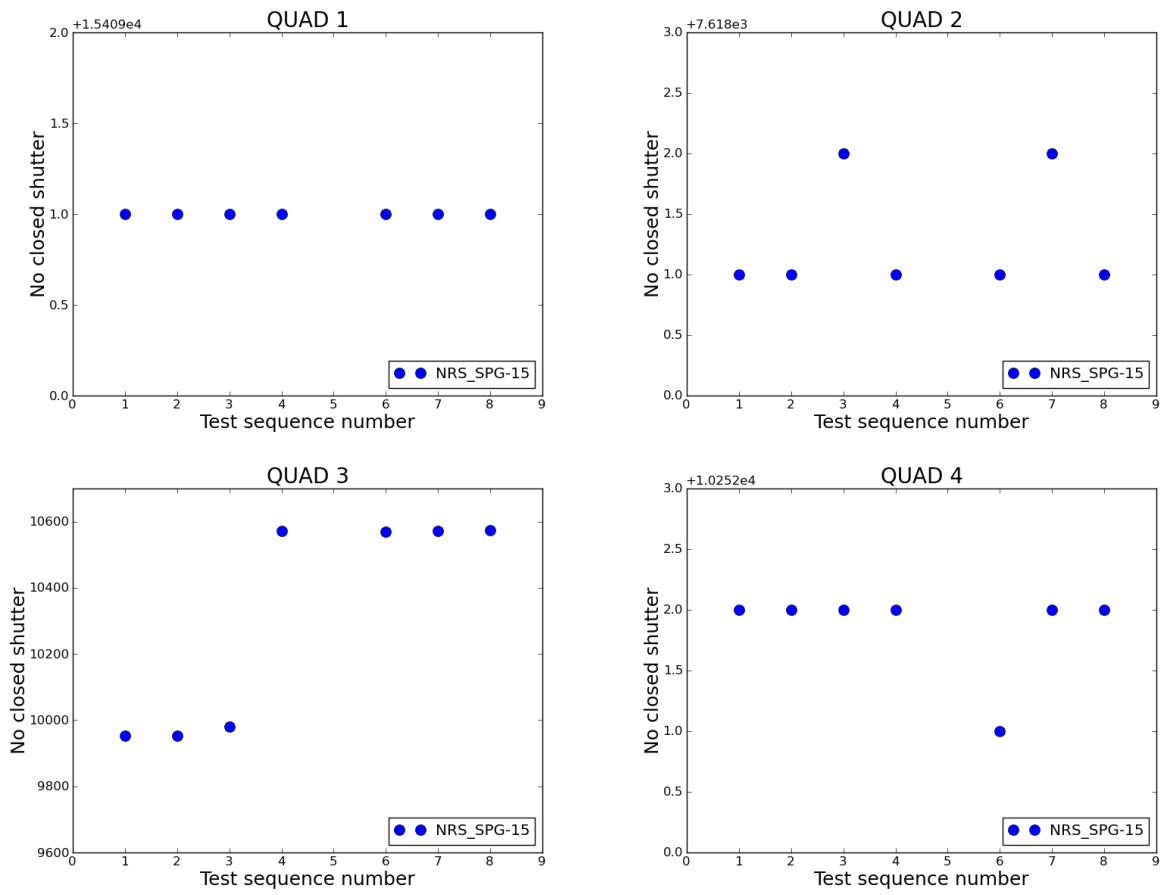


Figure 6: Number of closed shutters in each MSA quadrant as a function of the exposure number within test sequence: SPG-15

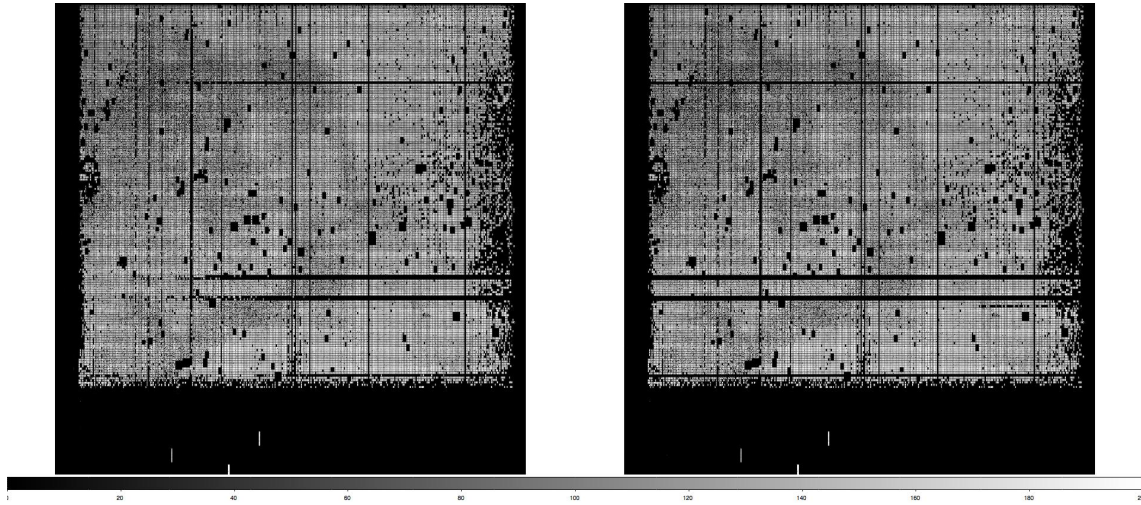


Figure 7: Images of quadrant 3 in the first exposure (left) and in the last exposure (right) of sequence SPG-15.

Giardino, G. 2012, MSA-detect tool, NIRSpec Technical Note NTN-2012-004, ESA/ESTEC available at <http://www.cosmos.esa.int/web/jwst/technical-notes>

APPENDIX

List of exposures analyzed here:

Sequence SPG-13

NRS_SPG-13-1-Q0-PP-A-Init_1_13725_JW1_jlab85_20130802T000748_20130802T001011
 NRS_SPG-13-2-Q1-PP-A-171VPP_2_13726_JW1_jlab85_20130802T001154_20130802T001419
 NRS_SPG-13-3-Q1-PP-A-365VPP_3_13727_JW1_jlab85_20130802T001533_20130802T001805
 NRS_SPG-13-4-Q2-PP-A-171VPP_4_13728_JW1_jlab85_20130802T002014_20130802T002243
 NRS_SPG-13-5-Q2-PP-A-365VPP_5_13729_JW1_jlab85_20130802T002406_20130802T002629
 NRS_SPG-13-6-Q3-PP-A-171VPP_6_13730_JW1_jlab85_20130802T002818_20130802T003047
 NRS_SPG-13-7-Q3-PP-A-365VPP_7_13731_JW1_jlab85_20130802T003236_20130802T003505
 NRS_SPG-13-8-Q4-PP-A-171VPP_8_13732_JW1_jlab85_20130802T003703_20130802T003932
 NRS_SPG-13-9-Q4-PP-A-365VPP_9_13733_JW1_jlab85_20130802T004107_20130802T004329
 NRS_SPG-13-10-Q0-PP-A-365ZPM_10_13734_JW1_jlab85_20130802T004511_20130802T004735
 NRS_SPG-13-11-Q0-PP-A-AOpen_12_13735_JW1_jlab85_20130802T004823_20130802T005049
 NRS_SPG-13-12-Q1-PP-A-365VPP_13_13736_JW1_jlab85_20130802T005213_20130802T005445
 NRS_SPG-13-13-Q2-PP-A-365VPP_14_13737_JW1_jlab85_20130802T005646_20130802T005913
 NRS_SPG-13-14-Q3-PP-A-365VPP_15_13738_JW1_jlab85_20130802T010250_20130802T010519
 NRS_SPG-13-15-Q4-PP-A-365VPP_16_13739_JW1_jlab85_20130802T010636_20130802T010905
 NRS_SPG-13-16-Q1-PP-A-171VPP_17_13740_JW1_jlab85_20130802T011039_20130802T011311
 NRS_SPG-13-17-Q2-PP-A-171VPP_18_13741_JW1_jlab85_20130802T011447_20130802T011719

NRS_SPG-13-18-Q3-PP-A-171VPP_19_13742_JW1_jlab85_20130802T011858_20130802T012124
NRS_SPG-13-19-Q4-PP-A-171VPP_20_13743_JW1_jlab85_20130802T012333_20130802T012605

Sequence SPG-15

NRS_SPG-15-1-Q3-SP-A-Init_1_13745_JW1_jlab85_20130802T014234_20130802T014503
NRS_SPG-15-2-Q3-SP-A-171VPP_6_13746_JW1_jlab85_20130802T014718_20130802T014940
NRS_SPG-15-3-Q3-SP-A-365VPP_7_13747_JW1_jlab85_20130802T015103_20130802T015327
NRS_SPG-15-4-Q3-SP-A-365ZPM_10_13748_JW1_jlab85_20130802T015421_20130802T015651
NRS_SPG-15-5-Q3-SP-A-TrgAcq_11_13749_JW1_jlab85_20130802T015724_20130802T020559
NRS_SPG-15-6-Q3-SP-A-AOpen_12_13750_JW1_jlab85_20130802T020629_20130802T020851
NRS_SPG-15-7-Q3-SP-A-365VPP_15_13751_JW1_jlab85_20130802T021055_20130802T021319
NRS_SPG-15-8-Q3-SP-A-171VPP_19_13752_JW1_jlab85_20130802T021504_20130802T021737

Sequence SPG-16

NRS_SPG-16-1-Q0-SP-A-Init_1_13753_JW1_jlab85_20130802T022120_20130802T022341
NRS_SPG-16-2-Q1-SP-A-171VPP_2_13754_JW1_jlab85_20130802T022526_20130802T022748
NRS_SPG-16-3-Q1-SP-A-365VPP_3_13755_JW1_jlab85_20130802T022912_20130802T023145
NRS_SPG-16-4-Q2-SP-A-171VPP_4_13756_JW1_jlab85_20130802T023321_20130802T023551
NRS_SPG-16-5-Q2-SP-A-365VPP_5_13757_JW1_jlab85_20130802T023727_20130802T023958
NRS_SPG-16-6-Q3-SP-A-171VPP_6_13758_JW1_jlab85_20130802T024143_20130802T024416
NRS_SPG-16-7-Q3-SP-A-365VPP_7_13759_JW1_jlab85_20130802T024539_20130802T024801
NRS_SPG-16-8-Q4-SP-A-171VPP_8_13760_JW1_jlab85_20130802T024959_20130802T025231
NRS_SPG-16-9-Q4-SP-A-365VPP_9_13761_JW1_jlab85_20130802T025409_20130802T025637
NRS_SPG-16-10-Q0-SP-A-365ZPM_10_13762_JW1_jlab85_20130802T025752_20130802T030023
NRS_SPG-16-11-Q0-SP-A-TrgAcq_11_13763_JW1_jlab85_20130802T030047_20130802T030919
NRS_SPG-16-12-Q0-SP-A-AOpen_12_13764_JW1_jlab85_20130802T030958_20130802T031223
NRS_SPG-16-13-Q1-SP-A-365VPP_13_13765_JW1_jlab85_20130802T031407_20130802T031638
NRS_SPG-16-14-Q2-SP-A-365VPP_14_13766_JW1_jlab85_20130802T031805_20130802T032036
NRS_SPG-16-15-Q3-SP-A-365VPP_15_13767_JW1_jlab85_20130802T032205_20130802T032433
NRS_SPG-16-16-Q4-SP-A-365VPP_16_13768_JW1_jlab85_20130802T032633_20130802T032901
NRS_SPG-16-17-Q1-SP-A-171VPP_17_13769_JW1_jlab85_20130802T033057_20130802T033329
NRS_SPG-16-18-Q2-SP-A-171VPP_18_13770_JW1_jlab85_20130802T033457_20130802T033725
NRS_SPG-16-19-Q3-SP-A-171VPP_19_13771_JW1_jlab85_20130802T033853_20130802T034120
NRS_SPG-16-20-Q4-SP-A-171VPP_20_13772_JW1_jlab85_20130802T034316_20130802T034538